Halli, Petteri; Elomaa, Heini; Wilson, Benjamin; Yliniemi, Kirsi; Lundström, Mari

Improved Metal Circular Economy-Selective Recovery of Minor Ag Concentrations from Zn Process Solutions

Published in:
ACS Sustainable Chemistry and Engineering

DOI:
10.1021/acssuschemeng.7b02904
10.1021/acssuschemeng.7b02904

Published: 01/01/2017

Document Version
Publisher's PDF, also known as Version of record

ACS Sustainable Chemistry & Engineering

Research Article

Cite This: ACS Sustainable Chem. Eng. 2017, 5, 10996-11004

pubs.acs.org/journal/ascecg

Improved Metal Circular Economy-Selective Recovery of Minor Ag Concentrations from Zn Process Solutions

Petteri Halli,[†] Heini Elomaa,[†] Benjamin P. Wilson,[†] Kirsi Yliniemi,[†,‡] and Mari Lundström*[,†]

[†]School of Chemical Engineering, Department of Chemical and Metallurgical Engineering, The Research Group of Hydrometallurgy and Corrosion, Aalto University, Vuorimiehentie 2, P.O. Box 16200, FI-00076 Aalto, Finland

[‡]School of Chemical Engineering, Department of Chemistry and Material Science, Aalto University, Kemistintie 1, P.O. Box 16100, FI-00076 Aalto, Finland

ABSTRACT: Silver is a metal widely applied in renewable energy applications and therefore subject to resource scarcity. The paper presents a new approach for recovering silver from zinc-containing solutions mimicking hydrometallurgical base metal process solution. By nature, silver present in ores or concentrates is more noble than zinc and not effectively leached into the sulfate media during zinc hydrometallurgical processing. This paper presents a novel approach for concentrating and recovering silver present in minor amounts in zinc sulfate media. The electrodeposition−redox replacement (EDRR) method was investigated in synthetic zinc sulfate solutions ([Zn] = 60 g/L, [Ag] = 1 ppb−250 ppm, [H_2SO_4] = 10 g/L) containing silver as low as 1 ppb. The deposited metal coating was analyzed by electrochemical techniques and SEM-EDS. As a result, an enrichment of silver as nano- and microparticles on electrodes was evident. With the application of multiple EDRR steps (n = 160), the method was shown to result in a high purity Ag layer (Ag/Zn ratio ≈ 1500 in the product) from solution with minor Ag content (Ag/Zn ratio ≈ 0.0017 in solution). Moreover, at the concentration levels studied, the EDRR method was shown to outperform conventional electrowinning (EW).

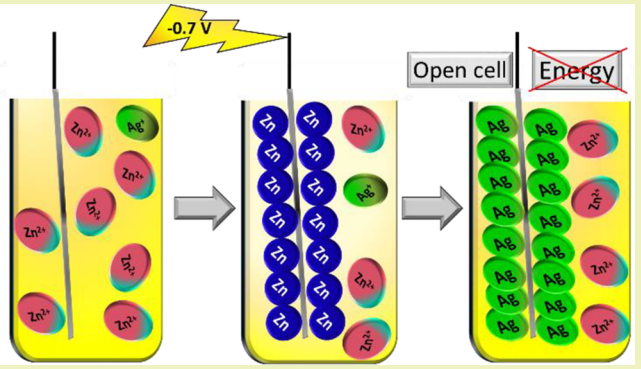

KEYWORDS: *EDRR, Silver recovery, Zinc process solution, Circular economy*

INTRODUCTION

There is a significant amount of impurities[1−4] present in the zinc ores and concentrates ending up in hydrometallurgical process solutions, end products, and leach residues.[5−7] Most of these impurities are base metals,[8,9], but noble metals, like silver and gold, can be also present. During the zinc electrowinning process, minor amount of the impurities end up in the electrolyte solution and can affect the purity of the deposited zinc cathode,[10] while most of the impurities are addressed in the solution purification stage. Fundamentally, silver present in the ore or concentrate[11−14] is in contact with sulfate solutions during hydrometallurgical processing, however, having only minor solubility (<200 ppm[15]) to the sulfate media. Moreover, typically the process conditions do not allow almost any silver dissolution. These kinds of base metal solutions are not conventionally considered as containing valuable metals and definitely not as sources for silver recovery.

Traditionally, cementation has been applied in hydrometallurgy for some impurity or side-product metal recovery from zinc sulfate solutions.[16] In the current study, the authors suggest that electrodepostion−redox replacement (EDRR) can provide a method for utilizing the cementation phenomenon in a more controlled manner. Although several authors have investigated redox replacement, the published research has primarily focused on building defect-free mono/multilayers and studying the behavior of surface-limited redox replacement (SLRR) from high purity chemicals with a relatively high noble metal content.[16−25] In addition, redox replacement (also called galvanic replacement or galvanic displacement) with electrodeposition has also been utilized in catalyst formation as shown, for example, in the recent review by Papaderakis et al.[26] The advantage of electrodeposition is that it allows easy tailoring of the process by different parameters such as deposition time and deposition rate (either by controlling potential or current). When combined with a redox replacement reaction, even more possibilities to control the enrichment become available as one has control over enrichment time simply by controlling the time for the redox replacement reaction. There is no published data on the EDRR method applied for metal recovery from industrial hydrometallurgical process and waste solutions. A few EDRR investigations about silver have been performed in synthetic solutions[27−29] in order to produce functional and defect free surfaces, but silver recovery and comprehensive investigations of EDRR in concentrated zinc sulfate solutions

Received: August 21, 2017
Published: September 26, 2017

DOI: 10.1021/acssuschemeng.7b02904
ACS Sustainable Chem. Eng. 2017, 5, 10996−11004

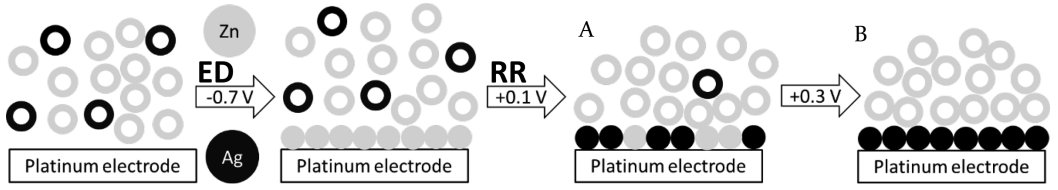

Figure 1. Schematic demonstration of EDRR procedure in zinc sulfate solution with minor amount of Ag present. Gray circles represent zinc and black ones silver. Empty gray and black circles represents zinc and silver ions in a solution, respectively, while filled circles represent metallic zinc and silver deposited on the surface either during ED or RR step. Diagram (A) demonstrates that with optimized parameters the layer consists of more Zn and less Ag, whereas diagram (B), with optimized parameters, shows that the surface is almost entirely Ag.

mimicking solutions typical for base metal production have not been conducted.

This work presents a method that provides a chemical free method for Ag recovery from hydrometallurgical-concentrated zinc sulfate solutions where silver is present only in minute concentrations. After EDRR of silver, the used electrodes can be removed from the solution in order to recover the deposited silver. Moreover, the silver is also in demand for other high-added materials such as antibacterial[30−32] or surface-enhanced Raman[33,34] surfaces. In this paper, the EDRR process parameters and the deposit quality will be investigated. In addition, the energy efficiency of the EDRR process is compared to that of electrowinning (EW), i.e., direct electrodeposition, to reveal the superiority of the EDRR approach.

As silver usage is ever increasing with the rising clean energy sector, silver is used, for example, as a connector in solar cells and batteries, and finding alternative raw material sources for silver is crucial if the clean energy sector is to take over for fossil fuels. This paper provides a new opening for the silver recovery from hydrometallurgical solutions, which have extremely low silver content, pushing circular economy thinking a step forward toward reality.

EXPERIMENTAL SECTION

Chemicals and Equipment. All the chemicals used in this work, $ZnSO_4{\cdot}7H_2O$ (Sigma-Aldrich), $AgNO_3$ (Sigma-Aldrich), and H_2SO_4 (VWR), were of technical grade, and the solutions were made using distilled water. Solutions consisted of a base metal (Zn) and a minority metal (Ag) in 10 g/L H_2SO_4 solution. The Zn concentration applied was 60 g/L in all the experiments, whereas the silver concentration was varied from 250 ppm to 1 ppb.

An IviumStat CompactStat (NL) potentiostat was employed for the electrochemical measurements, and SEM-EDS (scanning electron microscope, Leo 1450 VP, Zeiss, Germany, Energy Dispersion Spectroscopy, INCA-Software, Oxford Instruments, UK) was used for product (deposition) analysis. The used acceleration voltage was 15 kV. Prior to SEM-EDS analysis, the samples were rinsed with distilled water and dried at room temperature. For each sample, between 10 to 20 spectra were measured and analyzed.

Cell Setup. The measurements were carried out in a three-electrode cell with a saturated calomel electrode (SCE, B521, SI Analytics) as a reference electrode, a Pt working electrode (WE) (0.4 cm^2), and a Pt counter electrode (CE) (having 15 times larger area compared to WE). The Pt substrate was 99.5% purity, having less than 500 ppm impurities of gold, silver, copper, and base metals (N.B. during the deposition analysis, these substrate impurities have been taken into account). Prior to each EDRR measurement, the Pt electrodes were cleaned in pure 10 g/L H_2SO_4 solution by a cyclic voltammetry (CV) measurement, where 10 cycles were performed with a scan rate of 50 mV/s starting from 0.0 V to +1.3 V, going to −0.3 V and back to 0.0 V vs SCE. After the cleaning procedure, the electrodes were thoroughly rinsed with distilled water before starting EDRR measurements. The same solution (10 g/L H_2SO_4) was also used as a base solution in which the silver deposition was investigated by observing the current density related to silver stripping (by CVs, + 0.3 V → + 1.0 V → −0.5 V → + 0.3 V vs SCE). All CV measurements were conducted with a scan rate of 20 mV/s. The solution volume was 40 ± 0.5 mL, and the distance between working and counter electrodes was 2 ± 0.1 cm.

EDRR and ED Measurements. The EDRR procedure consisted of two steps: Step 1 was an electrodeposition (ED) step during which a constant deposition potential (E_1) was applied on the electrode for a predetermined time (t_1). Step 2, i.e., the redox replacement (RR) step, followed immediately after the electrodeposition step. During the RR step, no external current or potential was applied, but the RR step continued until the open circuit potential (OCP) reached a predetermined cutoff potential E_2 or cutoff time t_2, which ever occurred first. The reactions occurring during Step 2 are similar to those traditionally considered as cementation in hydrometallurgy. After the redox replacement step, a new electrodeposition step commenced without delay, and cycling between Step 1 and Step 2 was performed.

In the current study, the EDRR parameters are as follows: E_1 was either −0.75 V, −0.70 V, or −0.65 V vs SCE, t_1 was 2, 4, 6, 8, 10, 20, or 40 s, E_2 was +0.25 V, + 0.30 V, or +0.35 V vs SCE, t_2 was 1000 s, and the number of cycles investigated was between 5 to 160.

During EDRR, Ag was enriched on the electrode surface from a solution containing a high concentration of Zn^{2+} ions and a low level of silver ions (Figure 1). During the electrodeposition step (Step 1), the zinc ions were reduced and deposited as Zn on the electrode. During the next step, i.e., redox replacement step (Step 2), the Zn layer was spontaneously replaced with the more noble silver metal ions still present in solution. Ag^+ oxidizes the deposited Zn, which dissolves back into the solution as Zn^{2+} ions, while Ag^+ ions were reduced to metallic Ag, resulting in an enrichment of silver on the surface. The spontaneous replacement takes place due to the difference in electrode potentials of Zn/Zn^{2+} and Ag/Ag^+: the electrode potential difference being ∼1.6 V between zinc and silver. After a full cycle, another cycle of EDRR was conducted, and the procedure was continued.

After each EDRR experiment, three cycles of CV were performed, and a Ag stripping peak was observed to identify successful enrichment of Ag on the Pt electrode (WE) as the current density is directly related to the deposited Ag amount.[35,36]

RESULTS AND DISCUSSION

EDRR Procedure: Parameter Optimization. Optimization experiments were conducted in a solution containing 60 g/L Zn, 100 ppm Ag, and 10 g/L H_2SO_4. First of all, the initial deposition potential of Zn (E_1) and cutoff potential (E_2) were determined from a CV measurement (Figure 2). The CV in Figure 2 indicates that Zn deposition started at approximately −0.55 V vs SCE, whereas the deposition of Ag (cutoff potential) occurs already at a potential of ca. E = 0.30 V vs SCE (inset, Figure 2). The stripping of Ag from the electrode surface starts at potentials >0.3 V vs SCE (Figure 2).

The deposition potentials (E_1) of −0.75, −0.70, and −0.65 V vs SCE were investigated. In all experiments, 10 EDRR cycles (n) were conducted, with a 10 s deposition time (t_1), and a

DOI: 10.1021/acssuschemeng.7b02904
ACS Sustainable Chem. Eng. 2017, 5, 10996−11004

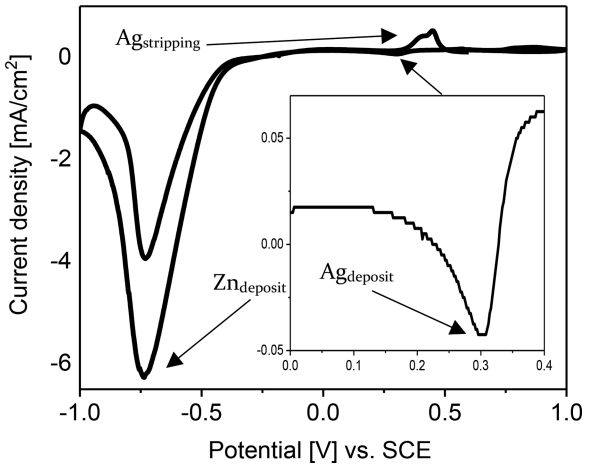

Figure 2. Average of nine (cycles 2 to 10) cyclic voltammetry measurements from 0.0 V → + 1.0 V → −1.0 V → 0.0 V (20 mV/s) in a solution containing 60 g/L Zn, 100 ppm Ag, and 10 g/L H_2SO_4 and a magnification of the silver deposition peak at +0.30 V vs SCE.

cutoff potential (E_2) of 0.30 V vs SCE (i.e., just before the Ag stripping peak) was employed. In order to evaluate the deposited amount of Ag on the electrode (i.e., the quality of the product), CV in the stripping region of Ag was conducted after the EDRR cycles, as shown in Figure 3A

It can be seen that utilizing deposition potentials (E_1) −0.75 V and −0.70 V vs SCE in EDRR resulted in a higher Ag recovery compared to E_1 = −0.65 V vs SCE. Furthermore, SEM-EDS analysis, performed after EDRR, also displayed a higher Ag/Zn ratio on the electrode surface when the deposition potential E_1 was −0.7 V vs SCE compared to E_1 = −0.65 V vs SCE (Table 1). SEM-EDS analysis suggested also that E_1 = −0.70 V was more favorable than −0.75 V, even though the Ag stripping peak in the CV measurements (Figure 3A) did not predict any difference between these two potentials. Moreover, an E_1 = −0.7 V vs SCE has a lower level of energy consumption when compared to E_1 = −0.75 V vs SCE.

Table 1. Weight Percentages of Zn and Ag Present on Electrode Surface after E_1 and E_2 Optimization Based on SEM-EDS Analysis (average of 10−20 point analysis)[a]

Potentials (vs SCE)	Zn (wt %)	Ag (wt %)	Ag/Zn
E_1 optimization			
$E_1 \rightarrow E_2$			
−0.65 V → + 0.30 V	0.17	16.34	97.7
−0.70 V → + 0.30 V	0.08	14.30	191
−0.75 V → + 0.30 V	3.97	26	6.6
E_2 optimization			
$E_1 \rightarrow E_2$			
−0.70 V → + 0.25 V	0.19	10.27	53.8
−0.70 V → + 0.30 V	0.08	14.30	191
−0.70 V → + 0.35 V	44.2	5.5	0.1

[a]In EDRR experiments, the solution had 60 g/L Zn, 100 ppm Ag, and 10 g/L H_2SO_4. Pt and its' impurities (substrate) are excluded from the results.

Figure 3B shows the CV data after cutoff (E_2) potential optimization (E_2 = +0.25, + 0.30, and +0.35 V in EDRR measurements). It can be seen that a value of E_2 = +0.25 V provided very low current density at silver stripping compared to + 0.30 V or +0.35 V vs SCE. Moreover, + 0.35 V was shown to be practically a too high cutoff potential as in these experiments the cutoff time (t_2) was reached before E_2 in every cycle. The SEM-EDS analysis (Table 1) confirms that the best Ag recovery (in terms of Ag:Zn ratio) was achieved with E_2 = +0.3 V vs SCE.

The optimization of deposition time (t_1) was conducted over a deposition time range of 2−40 s. Figure 4 shows that the Ag stripping peak height increased up to 10 s, after which the peak current density initially started to decrease before subsequently increasing again. The most favorable deposition time (10 s) provides an optimal level of Zn deposition for Ag to replace. The redox replacement reaction takes place only at the deposit/solution interface, and thus, a thin layer with a certain level of defects will favor the Ag enrichment. With a higher deposition time (20 s), the thickness of the deposited Zn layer increases (during the ED step), resulting in a lower Ag peak current density (Figure 4). After longer deposition times (30 and 40 s),

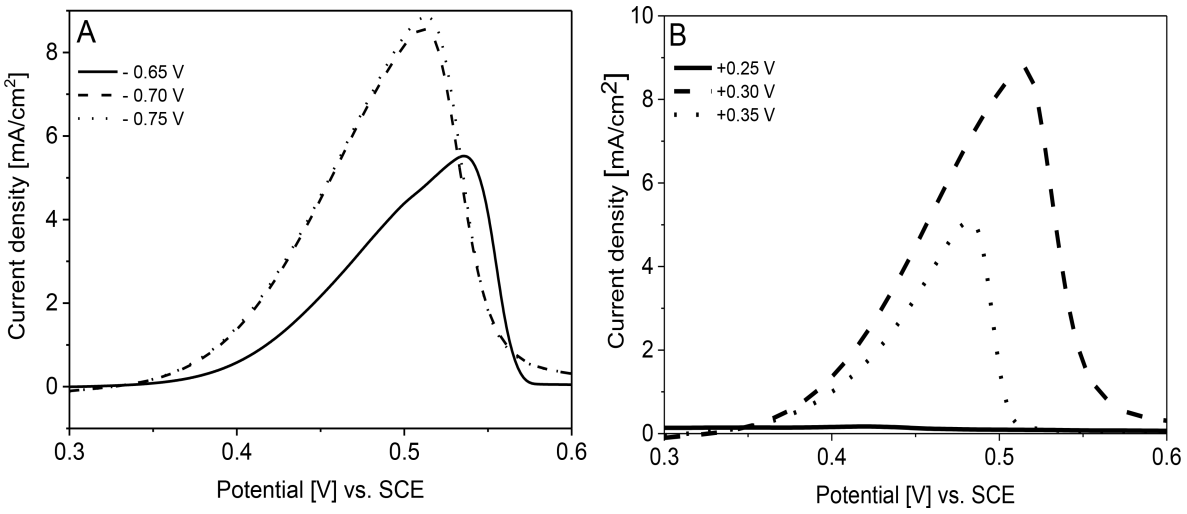

Figure 3. Ag peak height of first CV cycle (+0.30 V → + 1.0 V → −0.5 V → + 0.30 V vs SCE) after (A) E_1 potential optimization (EDRR parameters 10 cycles, E_2 = +0.30 V vs SCE) and (B) E_2 potential optimization (EDRR parameters n = 10 cycles, E_1 = −0.70 V vs SCE) in a solution containing 60 g/L Zn, 100 ppm Ag, and 10 g/L H_2SO_4.

DOI: 10.1021/acssuschemeng.7b02904
ACS Sustainable Chem. Eng. 2017, 5, 10996−11004

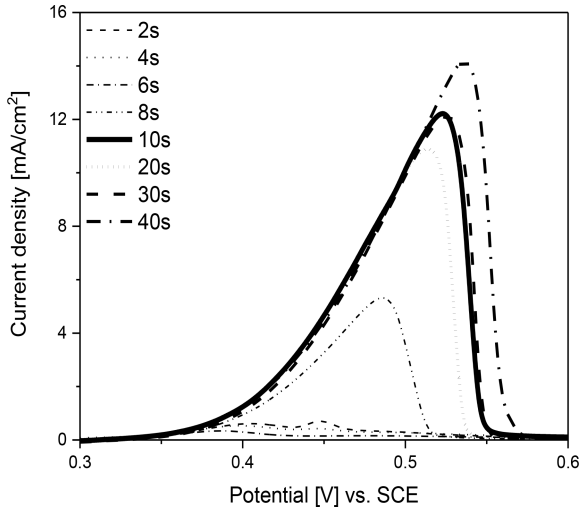

Figure 4. Ag peak height of the first CV + (0.3 V → + 1.3 V → −0.3 V → + 0.3 V vs SCE) of t_1 deposition time optimization (EDRR parameters 10 cycles, E_1 = −0.70 V and E_2 = +0.30 V vs SCE) in a solution containing 60 g/L Zn, 100 ppm Ag, and 10 g/L H_2SO_4.

higher Ag stripping peaks were observed but also an increased level of H_2 evolution. H_2 evolution was shown to decrease the surface uniformity due to H_2 formation, as highlighted by the light color spots evident in Figure 5. H_2 evolution is also not

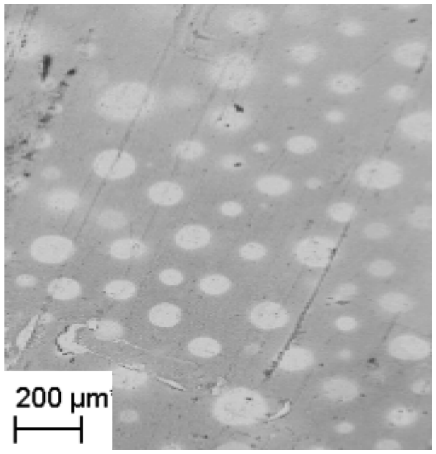

Figure 5. SEM micrograph of the effect of hydrogen evolution (round lighter color spots) on the surface morphology. EDRR parameters t_1 = 20s, n = 10 cycles, and E_1 = −0.70 V and E_2 = +0.30 V vs SCE. The electrode was employed during longer deposition ($t_1 \geq$ 20s) times.

favored during the process as it reduces the overall energy efficiency. Furthermore, all deposition times higher than 10 s were shown to compromise the purity of the deposit as more zinc remained under the redox replaced silver layer, as shown in Table 2. Therefore, optimum deposition time (t_1) was determined as 10 s.

Figure 6A shows the typical behavior of the electrode potential during the process, and Figure 6B shows the average current density used per cycle during EDRR measurements (E_1 = −0.7 V vs SCE, t_1 = 10 s, cutoff E_2 = 0.3 V vs SCE, n = 10 cycles). The current density varies as more silver layers are formed on the surface of the electrode, as the formation of each new layer of zinc—on top of the previous silver rich layer—requires less energy than the previous one.

Table 2. Weight Percentages of Zn and Ag Present on Electrode Surface after t_1 Optimization Based on SEM-EDS Analysis (average of 10−20 point analysis)[a]

Deposition time (t_1) (s)	Zn (wt %)	Ag (wt %)	Ag/Zn
2	0.26	4.49	17
6	0.23	7.96	34
10	0.08	14.30	190
20	0.30	25.15	85
40	0.26	26	100

[a]The solution had 60 g/L Zn, 100 ppm Ag, and 10 g/L H_2SO_4. Pt is excluded from the results.

The results showed that the time required for each redox replacement step decreased with an increased number of steps as more silver was deposited on the surface. When a few silver atoms are deposited on the surface of the electrode, silver will more easily nucleate there due to the spontaneous RR effect, observed previously for other EDRR or surface-limited redox replacement measurements.[37] On the other hand, the diffusion of silver ions to the surface at some point starts to control the rate of replacement, and it is these two phenomena that usually determine the total length of EDRR measurements. The issue of diffusion limitation can be ameliorated by enhancing mass transfer in the setup, for example, by either continuous solution stirring. or pumping.

Recovery of Minor Concentrations of Ag. In order to investigate more realistic industrial-type solutions, the effect of Ag concentration on the levels of deposited silver was investigated over a wide Ag concentration range (1 ppb−250 ppm).

[Ag] = 1 − 1000 ppb. In accordance with the previously optimized EDRR parameters outlined above, the experimental limits were kept at t_1 = 10 s, E_1 = −0.70 V, and E_2 = +0.30 V vs SCE and 10 EDRR cycles (n) in order to investigate the effect of silver concentration. Figure 7 presents the EDRR measurement data for solutions with 1 000, 500, 50, and 1 ppb of Ag. From these results, it can be seen that with decreasing Ag concentration the RR time increases, a fact that is also highlighted in Figure 8.

With minute Ag concentrations (1−1000 ppb), the electrochemical analysis (CV) did not give a clear Ag stripping peak at the anodic side; therefore, the platinum electrodes were investigated by SEM-EDS (Table 3). According to SEM-EDS analysis, the amount of silver enrichment was significant (Ag to Zn ratios in the deposit were determined to vary from 2 to nearly 30 once the background impurities present in the Pt electrode were excluded from the raw data) even at very low Ag (1 ppb) content in the solution. This is an exceptionally good recovery and shows that the EDRR method presented can truly be utilized in solutions previously considered to be uneconomic when it comes to the recovery of Ag and other more noble metals.

[Ag] = 5 − 250 ppm. Figure 9 presents the current densities obtained at the silver stripping peak when the concentration of Ag was varied from 5 to 250 ppm. As expected, the Ag stripping peak height increases with an increase in Ag concentration up to 100 ppm. At 250 ppm, a slight change in the peak shape can be observed, with the peak area being of the same magnitude as that recorded for 100 ppm. The electrodes employed were also investigated by SEM-EDS, and the results are displayed in Table 4. It was found that although the amount of zinc deposited on the electrode

DOI: 10.1021/acssuschemeng.7b02904
ACS Sustainable Chem. Eng. 2017, 5, 10996−11004

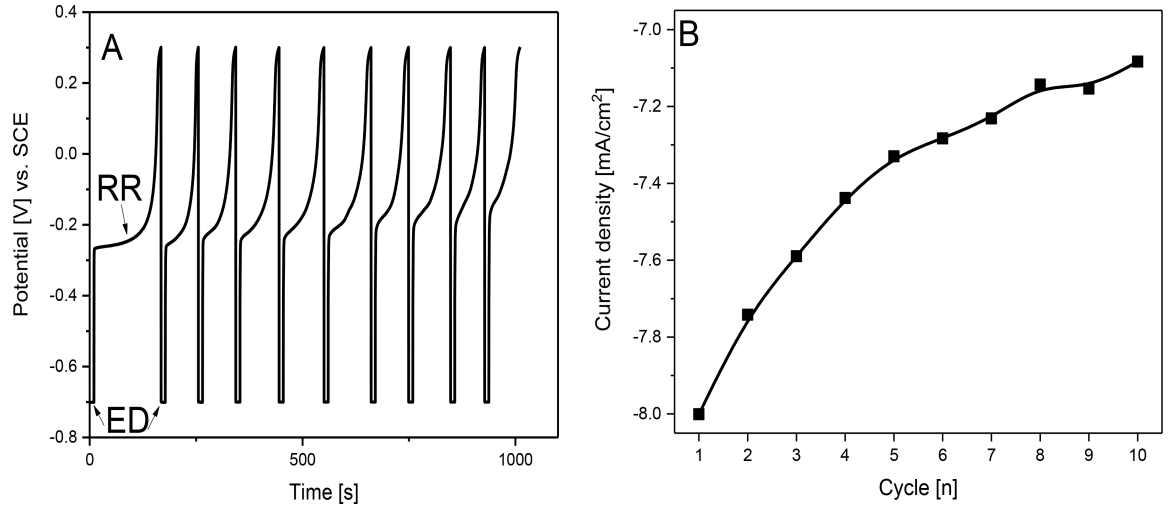

Figure 6. (A) Typical electrode potential behavior and (B) average current density as a function of EDRR cycles (n) in a solution with 60 g/L Zn, 100 ppm Ag, and 10 g/L H_2SO_4. EDRR parameters used were E_1 = −0.70 V and E_2 = +0.30 V vs SCE, t_1 = 10 s, and n = 10.

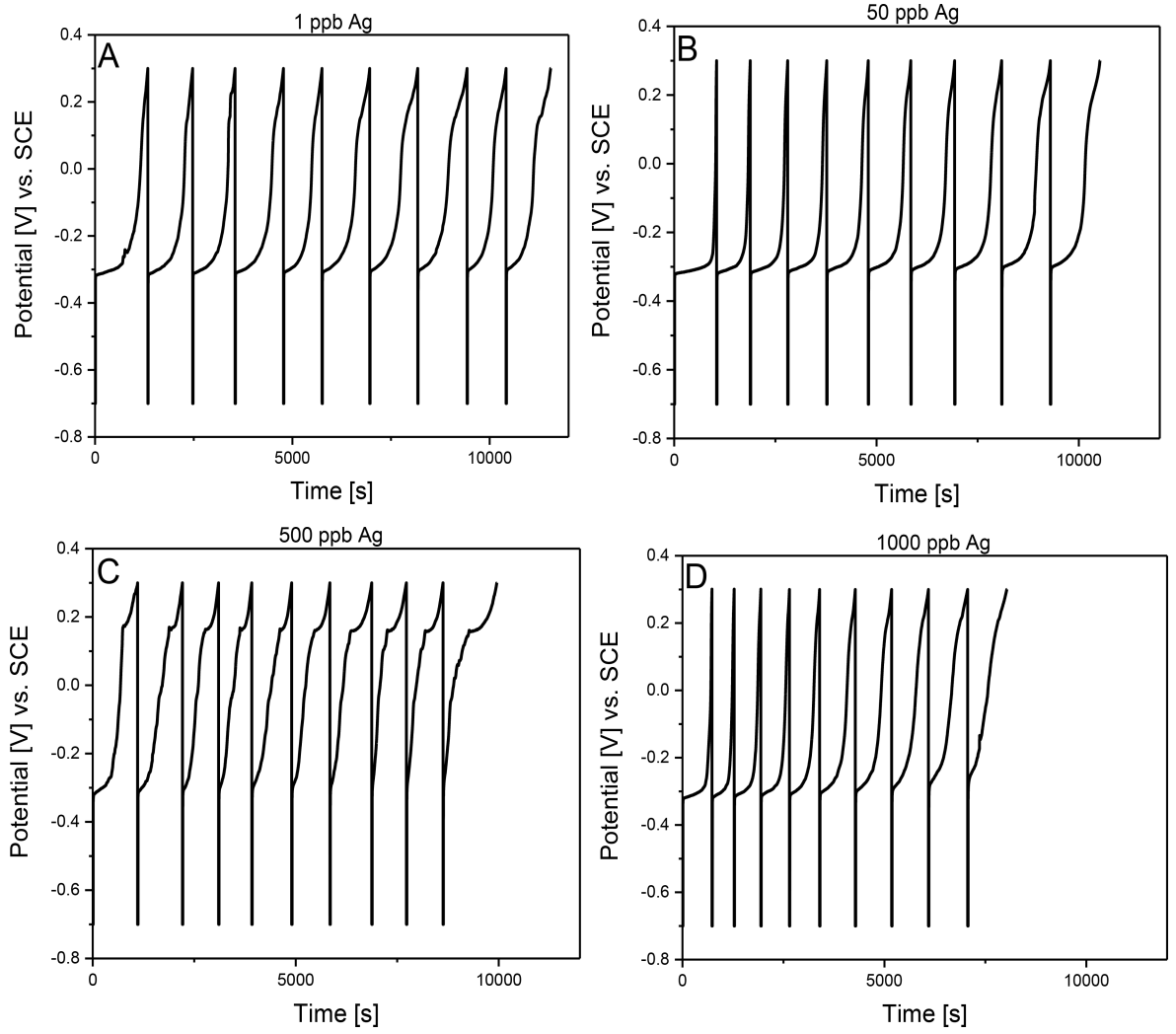

Figure 7. Potential profile of WE during EDRR measurements in 60 g/L Zn and 10 g/L H_2SO_4 solution containing (A) 1 ppb Ag, (B) 50 ppb Ag, (C) 500 ppb Ag, and (D) 1000 ppb Ag, respectively. EDRR parameters were E_1 = −0.70 V and E_2 = +0.30 V vs SCE, t_1 = 10 s, and n = 10.

surfaces did not show much variation the content of silver in the surface deposit was enhanced with increased Ag solution concentration, resulting in higher Ag/Zn ratios, which is also demonstrated in Figure 10.

DOI: 10.1021/acssuschemeng.7b02904
ACS Sustainable Chem. Eng. 2017, 5, 10996−11004

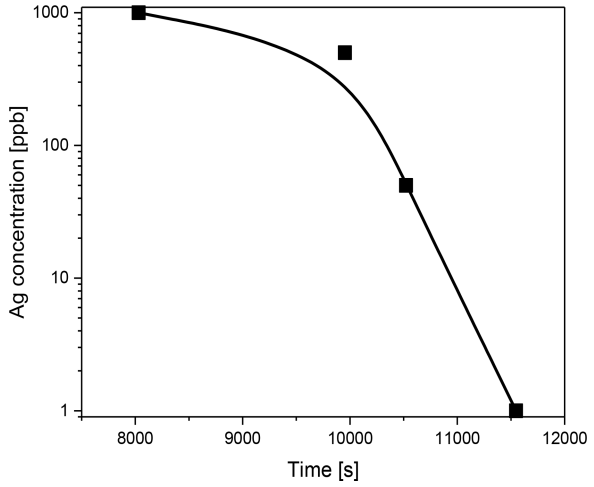

Figure 8. Time needed to complete EDRR measurements (E_1 = −0.70 V and E_2 = +0.30 V vs SCE, t_1 = 10 s, and n = 10) in solutions containing 60 g/L Zn, 10 g/L H_2SO_4, and 1000, 500, 50, and 1 ppb Ag.

Table 3. Weight Percentages of Zn and Ag Present on Electrode Surface Based on SEM-EDS Analysis (average of 10−20 point analysis[a]

	Product analysis (SEM-EDS)		
Ag content in the solution (ppb)	Zn (wt %)	Ag (wt %)	Ag/Zn
1	0.03	0.18	6
50	0.04	1.10	28
500	0.03	0.33	11
1000	0.13	0.33	2.5

[a]The solution had 60 g/L Zn, 10 g/L H_2SO_4, and varied Ag concentration from 1 to 1 000 ppm. Pt is excluded from the results.

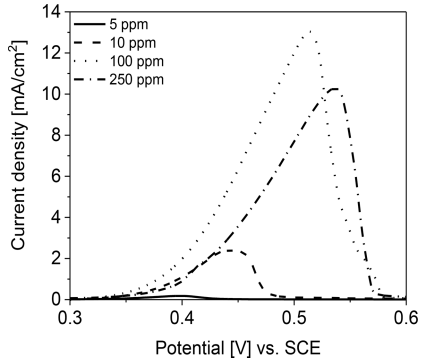

Figure 9. Silver stripping peaks after the EDRR experiments in solutions (60 g/L Zn and 10 g/L H_2SO_4) with varying silver content (5−250 ppm), E_1 = −0.70 V and E_2 = +0.30 V vs SCE, t_1 = 10 s, and n = 10.

Product Quality as a Function of Time. The effect of EDRR cycles (n) were investigated in a solution containing 60 g/L Zn, 100 ppm Ag, and 10 g/L H_2SO_4. The studied range of the cycles varied between 10 to 160. In Figure 11 is presented the obtained EDRR measurement data when n = 160 was conducted. As can be seen, in the absence of constant solution changing or stirring, the available Ag ions are consumed after n = 160, presenting a threshold value for Ag recovery in the investigated environment by batch operation.

Table 4. Weight Percentages of Zn and Ag Present on Electrode Surface Based on SEM-EDS Analysis (average of 10−20 point analysis). The solution had 60 g/L Zn, 10 g/L H_2SO_4, and varied Ag concentration from 5 to 250 ppm[a]

Ag content in the solution (ppm)	Zn (wt %)	Ag (wt %)	Ag/Zn
5	0.20	0.84	4.0
10	0.07	4.94	71
100	0.08	14.30	180
250	0.06	38.67	640

[a]N.B. Effect of the Pt electrode is excluded from the results.

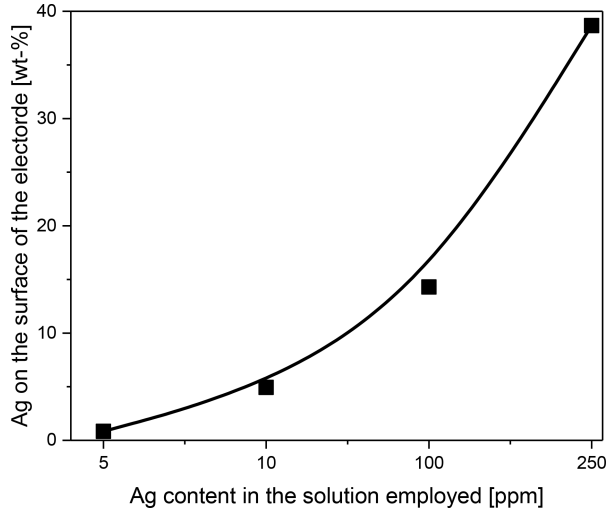

Figure 10. Amount of deposited silver as a function of original Ag content in the solution containing 60 g/L Zn and 10 g/L H_2SO_4. EDRR parameters used were E_1 = −0.70 V and E_2 = +0.30 V vs SCE, t_1 = 10 s, and n = 10.

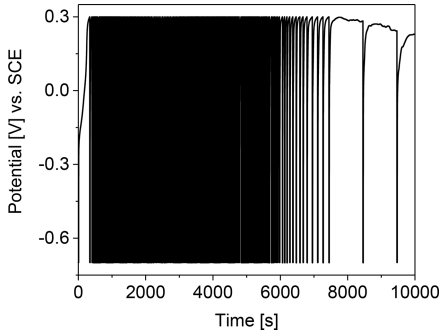

Figure 11. EDRR measurement data obtained when 160 EDRR cycles were employed in a solution containing 60 g/L Zn, 100 ppm Ag, and 10 g/L H_2SO_4. E_1 = −0.70 V and E_2 = +0.30 V vs SCE and t_1 = 10 s.

The amount of Ag deposited on the surface of the electrode by n = 25−160 was investigated by SEM-EDS, and the results are shown in Table 5. It can be observed that with increased process time in the form of cycling (n) the content of deposited Ag also increased exponentially to become the dominating element of the electrode, while conversely, the amount of deposited Zn decreased exponentially as a function of cycles conducted. This result confirms that the investigated novel approach for Ag recovery by EDRR can result in a high quality Ag product even with longer cycling times.

Deposition Mechanism and Surface Morphology. The deposition of silver was found to occur in small clusters on the surface of the platinum electrode (Figure 12A) due to the

DOI: 10.1021/acssuschemeng.7b02904
ACS Sustainable Chem. Eng. 2017, 5, 10996−11004

Table 5. Weight Percentages of Zn and Ag Present on Electrode Surface Based on SEM-EDS Analysis (average of 10−20 point analysis)[a]

Amount of cycles (n)	Zn (wt-%)	Ag (wt-%)	Ag/Zn
25	2.69	21.43	8.0
50	1.72	21.36	12
100	0.25	21.79	86
160	0.05	69.13	1500

[a]The solution had 60 g/L Zn, 100 ppm Ag, and 10 g/L H_2SO_4. N.B. Effect of the Pt electrode is excluded from the results.

nucleation of zinc which begins at inhomogeneities on the platinum electrode surface where a higher surface energy exists.[37,38] As silver enrichment takes place via a redox replacement reaction of zinc, it follows that this enrichment will show similar profiles to that of zinc. In Figure 12B, the interface at the platinum electrode and deposited silver can be observed. Here, a continuous silver layer has been deposited on the edge of the electrode. The deposition of silver was found to follow the same process regardless of the concentration of silver used. The formed electrodeposited layer contained a relatively low amount of zinc compared to the silver (Tables 1−5), and the whole layer was observed to be porous in nature regardless of the silver contents utilized.

Comparison of EDRR and EW. As demonstrated by both the SEM-EDS and CV measurements, EDRR was proven to be a powerful method for enriching silver from solutions in which Ag is present at low concentrations, even below the solution analysis limit (1 ppb). Figure 13 compares the advantage of EDRR over electrowinning (EW) in a solution containing 60 g/L Zn, 100 ppm Ag, and 10 g/L H_2SO_4. The parameters used were such that the applied electrodeposition time was double the duration in EW comparefd to that used in EDRR: the parameters for EDRR were E_1 = −0.70 V and E_2 = +0.30 V vs SCE, t_1 = 10 s, and n = 10, and for EW were t = 200s, E = +0.3 V vs SCE, and n = 1. The Ag stripping peak height obtained with EDRR was shown to be significantly larger when compared to the Ag stripping peak obtained after the EW experiment (Figure 13), even though the energy used for EW was double that used for EDRR (200 s vs 10 times 10 s), showing the great potential of EDRR in silver enrichment. The SEM-EDS analysis indicated that approximately a 20 times higher product quality (Ag/Zn ratio 230 vs 11) was achieved when using EDRR compared to EW (Table 6).

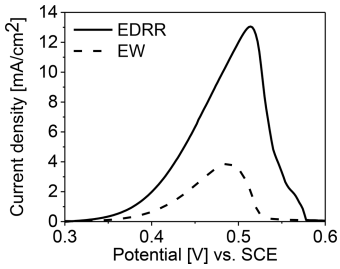

Figure 13. Comparison between EDRR and EW in a solution containing 60 g/L Zn, 100 ppm Ag, and 10 g/L H_2SO_4. EDRR parameters were E_1 = −0.70 V and E_2 = +0.30 V vs SCE, t_1 = 10 s, and n = 10, and EW parameters were t = 200s, E = +0.30 V, and n = 1.

Table 6. Weight Percentages of Zn and Ag Present on Electrode Surface Based on SEM-EDS Analysis (average of 10−20 point analysis)[a]

Method	Zn (wt %)	Ag (wt %)	Ag/Zn
EDRR	0.10	23.35	230
EW	0.08	0.87	11

[a]The solution had 60 g/L Zn, 100 ppm A,g and 10 g/L H_2SO_4. Pt is excluded from the results.

CONCLUSIONS

In this study, an electrodeposition−redox replacement (EDRR) method was used for the successful Ag enrichment from solutions with high zinc content (60 g/L) and extremely low silver content (even as low as 1 ppb) in sulfate media. Such concentrations are typical for hydrometallurgical zinc process solutions—not considered generally to be a source of valuable metals—and as such, this paper outlines a novel approach for using these solutions as raw materials for silver recovery. EDRR was conducted over a wide range of silver concentrations (1 ppb−250 ppm) in order to draw comprehensive conclusions about the functionality of spontaneous redox replacement for Ag recovery. The optimized parameters for Zn and Ag EDRR were found to be E_1 = −0.70 and E_2 = +0.30 V vs SCE and t_1 = 10 s.

The results suggest that Ag concentrations as low as 1 ppb can be recovered from concentrated Zn sulfate solutions by EDRR. Furthermore, SEM-EDS confirmed the enrichment of silver on the surface of a platinum electrode at all silver concentrations investigated. The time required to complete the

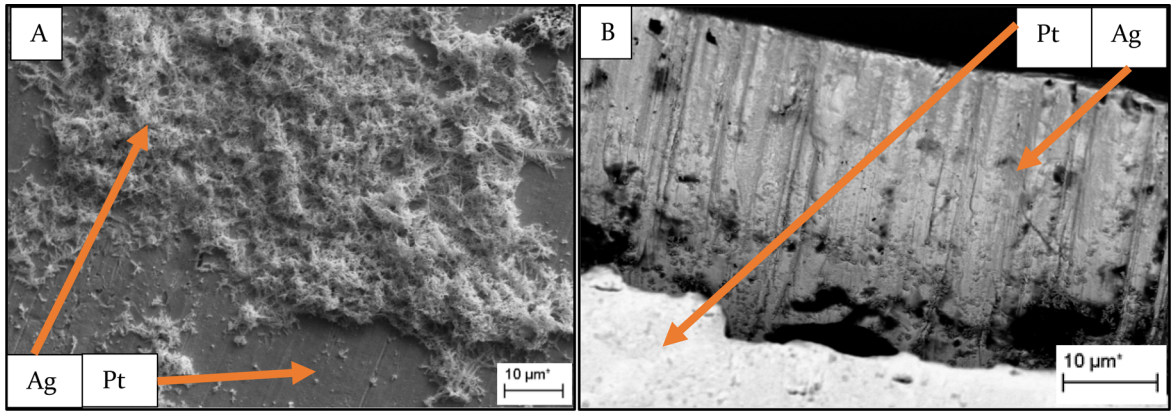

Figure 12. Secondary electron A (SE) and back scattered electron B (BSE) micrographs of silver deposition on the platinum electrode (A) at the center and (B) at the edge (60 g/L Zn, 250 ppm Ag, 10 g/L H_2SO_4, E_1 = −0.70 V and E_2 = +0.30 V vs SCE, t_1 = 10 s, and n = 10).

DOI: 10.1021/acssuschemeng.7b02904
ACS Sustainable Chem. Eng. 2017, 5, 10996−11004

EDRR cycle was shown to decrease when the content of Ag in the solution was increased. The resultant Ag layer deposited was also found to be porous but still rich in Ag.

Moreover, EDRR was shown to be more energy efficient when compared to conventional silver electrowinning (EW), especially at lower Ag concentrations. The results indicated that the energy required for EW is significantly higher when compared to that needed for EDRR, while conversely the quality of the product (Ag/Zn ratio) was shown to be 20 times higher compared to EW. Furthermore, the energy efficiency and feasibility of EDRR make it an extremely competitive method for silver recovery from side streams of hydrometallurgical processes, and thus, it can have a remarkable impact in the field of circular economy.

AUTHOR INFORMATION

Corresponding Author

*E-mail: mari.lundstrom@aalto.fi.

ORCID

Petteri Halli: 0000-0002-1803-7632

Benjamin P. Wilson: 0000-0002-2874-6475

Kirsi Yliniemi: 0000-0003-2536-388X

Author Contributions

The manuscript was written through contributions of all authors.

Notes

The authors declare no competing financial interest.

ACKNOWLEDGMENTS

This work has been financed by the Association of Finnish Steel and Metal Producers (*METSEK-project*) and "*NoWASTE*" project (Grant 297962) funded by Academy of Finland. The research also made use of the Academy of Finland funded "*RawMatTERS Finland Infrastructure*" (RAMI) based at Aalto University.

ABBREVIATIONS

EDRR	electrodeposition−redox replacement
CV	cyclic voltammetry
EW	electrowinning
SEM-EDS	scanning electron microscope-energy dispersion spectroscopy
SLRR	surface-limited redox replacement
WE	working electrode
CE	counter electrode
SCE	saturated calomel electrode.

REFERENCES

(1) Qin, W. Q.; Li, W. Z.; Lan, Z. Y.; Qiu, G. Z. Simulated small-scale pilot plant heap leaching of low-grade oxide zinc ore with integrated selective extraction of zinc. *Miner. Eng.* **2007**, *20* (7), 694−700.

(2) Xu, H.; Wei, C.; Li, C.; Fan, G.; Deng, Z.; Zhou, X.; Qiu, S. Leaching of a complex sulfidic, silicate-containing zinc ore in sulfuric acid solution under oxygen pressure. *Sep. Purif. Technol.* **2012**, *85*, 206−212.

(3) Ault, A. R.; Frazer, E. J. Effects of certain impurities on zinc electrowinning in high-purity synthetic solutions. *J. Appl. Electrochem.* **1988**, *18* (4), 583−589.

(4) Maja, M.; Spinelli, P. Detection of metallic impurities in acid zinc plating baths. *J. Electrochem. Soc.* **1971**, *118* (9), 1538−1540.

(5) Ju, S.; Zhang, Y.; Zhang, Y.; Xue, P.; Wang, Y. Clean hydrometallurgical route to recover zinc, silver, lead, copper, cadmium and iron from hazardous jarosite residues produced during zinc hydrometallurgy. *J. Hazard. Mater.* **2011**, *192* (2), 554−558.

(6) Kangas, P.; Koukkari, P.; Wilson, B. P.; Lundström, M.; Rastas, J.; Saikkonen, P.; Leppinen, J.; Hintikka, V. *Hydrometallurgical Processing of Jarosite to Value-Added Products*; Conference in Minerals Engineering, Luleå, Sweden, Feb. 7−8, 2017.

(7) Koukkari, P.; Kangas, P.; Nyström, M.; Lundström, M.; Wilson, B.; Rastas, J.; Saikkonen, P. *Jarogain Process for Recovering Value-Added Metals from RLE Zinc Residue*; ALTA2017, Perth, Australia, May 20−27, 2017, Uranium-REE Sessions.

(8) Fukubayashi, H. The effect of Impurities and Additives on the Electrowinning of Zinc. Ph.D. Thesis, Missouri University of Science and Technology, 1972.

(9) Fosnacht, D. R.; O'Keefe, T. J. The effects of certain impurities and their interactions on zinc electrowinning. *Metall. Trans. B* **1983**, *14* (4), 645−655.

(10) Mureşan, L.; Maurin, G.; Oniciu, L.; Gaga, D. Influence of metallic impurities on zinc electrowinning from sulphate electrolyte. *Hydrometallurgy* **1996**, *43* (1−3), 345−354.

(11) Wang, X. Q.; Xie, K. Q.; Ma, W. H.; Yang, M. Y.; Zeng, P.; Cao, Y. C. Recovery of zinc and other valuable metals from zinc leach residue by top blowing fuming method. *Trans. Inst. Min. Metall., Sect. C* **2013**, *122* (3), 174−178.

(12) Lew, R. W.; Dreisinger, D. B.; Gonzalez-Dominguez, J. *The Removal of Cobalt from Zinc Sulphate Electrolytes Using the Cu-Sb Process: Kinetics, Mechanisms and Morphological Characterisation*, World Zinc '93: Proceedings of the International Symposium on Zinc, Hobart, Tasmania, Oct. 10−13, 1993.

(13) Mureşan, L.; Maurin, G.; Oniciu, L.; Avram, S. Effects of additives on zinc electrowinning from industrial waste products. *Hydrometallurgy* **1996**, *40* (3), 335−342.

(14) Venkateswaran, K. V.; Srinivasan, G. N.; Nandakumar, V. Electrowinning of zinc-Effect of metallic impurities and addition agents. *Bull. Electrochem.* **1996**, *12* (5), 349−351.

(15) Morrison, R. M. The dissolution of silver in ferric sulphate-sulphuric acid media. *Hydrometallurgy* **1989**, *22* (1−2), 67−85.

(16) Salminen, J.; Riihimäki, T.; Ruonala, M. Method for Treating a Solution Containing Zinc Sulphate. U.S. Patent No. 9,617,621, Apr. 11, 2017.

(17) Fayette, M.; Liu, Y.; Bertrand, D.; Nutariya, J.; Vasiljevic, N.; Dimitrov, N. From Au to Pt via surface limited redox replacement of Pb UPD in one-cell configuration. *Langmuir* **2011**, *27* (9), 5650−5658.

(18) Gokcen, D.; Bae, S. E.; Brankovic, S. R. Stoichiometry of Pt submonolayer deposition via surface-limited redox replacement reaction. *J. Electrochem. Soc.* **2010**, *157* (11), D582−D587.

(19) Qu, D.; Lee, C. W. J.; Uosaki, K. Pt nano-layer formation by redox replacement of Cu adlayer on Au (111) surface. *Bull. Korean Chem. Soc.* **2009**, *30* (12), 2875−2876.

(20) Mkwizu, T. S.; Mathe, M. K.; Cukrowski, I. Electrodeposition of multilayered bimetallic nanoclusters of ruthenium and platinum via surface-limited redox− replacement reactions for electrocatalytic applications. *Langmuir* **2010**, *26* (1), 570−580.

(21) Mrozek, M. F.; Xie, Y.; Weaver, M. J. Surface-enhanced Raman scattering on uniform platinum-group overlayers: Preparation by redox replacement of underpotential-deposited metals on gold. *Anal. Chem.* **2001**, *73* (24), 5953−5960.

(22) Kim, Y. G.; Kim, J. Y.; Vairavapandian, D.; Stickney, J. L. Platinum nanofilm formation by EC-ALE via redox replacement of UPD copper: Studies using in-situ scanning tunneling microscopy. *J. Phys. Chem. B* **2006**, *110* (36), 17998−18006.

(23) Sarkar, A.; Manthiram, A. Synthesis of Pt@ Cu core− shell nanoparticles by galvanic displacement of Cu by Pt4+ ions and their application as electrocatalysts for oxygen reduction reaction in fuel cells. *J. Phys. Chem. C* **2010**, *114* (10), 4725−4732.

(24) Wragg, D. A.; Yliniemi, K.; Watson, T. M.; Worsley, D. A. Platinized counter electrodes for dye sensitized solar cells through the redox replacement of a low power electrodeposited lead sacrificial template. *ECS Trans.* **2013**, *53* (24), 11−17.

DOI: 10.1021/acssuschemeng.7b02904
ACS Sustainable Chem. Eng. 2017, 5, 10996−11004

(25) Yliniemi, K.; Wragg, D.; Wilson, B. P.; McMurray, H. N.; Worsley, D. A.; Schmuki, P.; Kontturi, K. Formation of Pt/Pb nanoparticles by electrodeposition and redox replacement cycles on fluorine doped tin oxide glass. *Electrochim. Acta* **2013**, *88*, 278−286.
(26) Papaderakis, A.; Mintsouli, I.; Georgieva, J.; Sotiropoulos, S. Electrocatalysts Prepared by Galvanic Replacement. *Catalysts* **2017**, *7* (3), 80.
(27) Herrero, E.; Buller, L. J.; Abruña, H. D. Underpotential deposition at single crystal surfaces of Au, Pt, Ag and other materials. *Chem. Rev.* **2001**, *101* (7), 1897−1930.
(28) Viyannalage, L. T.; Vasilic, R.; Dimitrov, N. Epitaxial growth of Cu on Au (111) and Ag (111) by surface limited redox replacement an electrochemical and STM study. *J. Phys. Chem. C* **2007**, *111* (10), 4036−4041.
(29) Brankovic, S. R.; Wang, J. X.; Adžić, R. R. Metal monolayer deposition by replacement of metal adlayers on electrode surfaces. *Surf. Sci.* **2001**, *474* (1), L173−L179.
(30) Chernousova, S.; Epple, M. Silver as antibacterial agent: ion, nanoparticle, and metal. *Angew. Chem., Int. Ed.* **2013**, *52* (6), 1636−1653.
(31) Le Ouay, B.; Stellacci, F. Antibacterial activity of silver nanoparticles: a surface science insight. *Nano Today* **2015**, *10* (3), 339−354.
(32) Cao, H.; Liu, X. Silver nanoparticles-modified films versus biomedical device-associated infections. *Wiley Interdiscip. Rev.: Nanomed. Nanobiotechnol.* **2010**, *2* (6), 670−684.
(33) Guo, S.; Wang, E. Noble metal nanomaterials: controllable synthesis and application in fuel cells and analytical sensors. *Nano Today* **2011**, *6* (3), 240−264.
(34) Rodriguez-Lorenzo, L.; Fabris, L.; Alvarez-Puebla, R. A. Multiplex optical sensing with surface-enhanced Raman scattering: a critical review. *Anal. Chim. Acta* **2012**, *745*, 10−23.
(35) Schaltin, S.; Vanhoutte, G.; Wu, M.; Bardé, F.; Fransaer, J. A QCM study of ORR-OER and an in situ study of a redox mediator in DMSO for Li−O 2 batteries. *Phys. Chem. Chem. Phys.* **2015**, *17* (19), 12575−12586.
(36) Jardy, A.; Lasalle-Molin, A. L.; Keddam, M.; Takenouti, H. Copper dissolution in acidic sulphate media studied by QCM and rrde under ac signal. *Electrochim. Acta* **1992**, *37* (12), 2195−2201.
(37) Kaischew, R.; Mutaftschiew, B. Electrolytic nucleation of mercury (in Germane). *Electrochim. Acta* **1965**, *10*, 643−650.
(38) Scharifker, B.; Hills, G. Theoretical and experimental studies of multiple nucleation. *Electrochim. Acta* **1983**, *28* (7), 879−889.

DOI: 10.1021/acssuschemeng.7b02904
ACS Sustainable Chem. Eng. 2017, 5, 10996−11004